DOI: 10.13009/EUCASS2019-163

Adaptive Control Allocation-based Control Design for Non-affine Morphing Aircraft System

Hanna Lee⋆*, Jihoon Lee*⋆*, Seong-hun Kim*⋆*, Seungyun Jung*⋆*, and Youdan Kim*⋆†
⋆*Seoul National University*
Seoul, Republic of Korea
hn.lee@snu.ac.kr · ydkim@snu.ac.kr
†Corresponding author

Abstract

A control design strategy is proposed for the variable span and sweep morphing wing aircraft considering the morphing parameters as control effectors, which makes the system non-affine in control. The system is differentiated to obtain an increased-order system, which is affine in the derivative of the control input. The frequency-apportioned control allocation is used to cover the control input frequency gap between control surfaces and morphing system. An adaptation law is used to compensate for the allocation error caused by the time-varying control effectiveness matrix. Numerical simulation is performed to demonstrate the effectiveness of the proposed scheme for a morphing wing aircraft.

1. Introduction

Recently, lots of studies on morphing aircraft have been conducted, because of the ability that the morphing aircraft can change its shape during flight, which allows the aircraft to perform various missions efficiently.[1,2] Owing to the large-scale shape change, the morphing aircraft has some benefits of extending the flight envelop, which improves maneuverability and controllability of the aircraft. Many control strategies on the morphing aircraft have been developed, which include linear quadratic regulator (LQR),[3] learning-based,[4] and adaptive control.[5] Most of these studies have considered the morphing parameter as an open-loop command, but those schemes have limits on maximizing the profit of morphing aircraft.

In the past decade, there has been significant progress in the area of control design for nonlinear system. Isidori[6] developed important results related to the geometric approach for analysis and control design of the nonlinear system. The problem of control of nonlinear system has also been addressed in the literature, and several control design procedures have been developed. Most of the control design methods developed in this context are applicable to the nonlinear system models that are linear in the unknown parameters and affine in control input u, that is, characterized by u appearing linearly in the state equation.

By considering the morphing parameters as additional control inputs, the system could have redundancy in control inputs, which is enabled to control the morphing parameters actively. The main challenging issue of this consideration is that the dynamic model of the system can be represented as a non-affine form in control input. If the control input is varied, the dynamic model also varies dependently to the control input. The control design for non-affine in control input system is a difficult problem. The dynamic nonlinearities in the morphing aircraft are dependent not only on the states of the system but also on the control inputs. Solving this problem with affine in control input system such as model approximation may lead to fatal degradation of control performance.[7]

Design of control systems for non-affine in control input system has not been studied much because of the difficulties involving control dependent nonlinearities.[8–11] A well-known approach to deal with this problem is to utilize the linearization of the nonlinear system model around an operating point.[12] Whereas the linearization may provide sufficiently good controllers around the operating point, accurate tracking of desired trajectories is not easy to achieve because the linearization results in a linear but time-varying model. Fixed linear controllers in such a case may result in unacceptable results. In this study, to overcome these problems, dynamic inversion based nonlinear methods are developed. Note that the dynamic inversion has been shown to be an efficient aircraft control method to tracking the desired dynamics.[13,14]

DOI: 10.13009/EUCASS2019-163

One of the main issues in the control design of non-affine in control input systems is how to solve the nonlinear algebraic equation in real-time. One nonlinear approach to deal with this problem was proposed that based on directly inverting the nonlinear function of the control input on a domain.[15] The method is based on a well-known idea of differentiating the original state equation, obtaining an augmented model linear in control derivative, and using it as a new control variable. For the case that it is difficult to invert the nonlinearity, the implicit function theorem[16] can be used to demonstrate the existence of the corresponding inverse function. Although the existence of an inverse function can be guaranteed by the implicit function theorem, it is generally difficult to prescribe a technique to actually obtain such an inverse.[17,18] In this study, nonlinear function in the control input is differentiated to obtain an increased-order system which is affine in the derivative of the control input. The derivative is then used as a virtual control variable, and the actual control input is computed via integration. However, this approach can be applied only to square dynamic systems of which numbers of states and control inputs are same. In addition, the strong assumption of the minimum phase system is required. When the flight path angle is selected as a regulated output to tracking reference trajectory, the dynamic model is represented as a non-minimum phase system, which results in unstable responses and the inverse is not guaranteed. To deal with this problem, the cascade control design scheme is introduced to achieve the tracking control for the non-square, non-minimum phase system.

Meanwhile, control allocation (CA) method is utilized to distribute the desired moments to the redundant control effectors of over-actuated system.[19] Various approaches of control allocation have been developed,[20,21] which include weighted pseudo-inverse method, daisy chain control allocation, direct control allocation, dynamic control allocation, and linear programming. In general, it can be assumed that the morphing parameters change slowly compared to the conventional control surfaces. In this case, rate difference of the control inputs should be considered to guarantee control performance. In this study, the frequency-apportioned control allocation (FACA) proposed by Davidson et al.[22] is used to account for the bandwidth gap between the control surfaces and morphing parameters. In addition, an adaptation law is used to compensate for the allocation error[23,24] caused by the time-varying control effectiveness matrix and the frequency-apportioned control allocation.

The objective of this study is to present a systematic approach of dynamic inversion based control scheme using adaptive frequency-apportioned control allocation (AFACA), which can be applied to non-affine, non-square nonlinear systems. By using adaptive frequency-apportioned control allocation method, the stability of the closed-loop system with respect to the model uncertainties is guaranteed. The system stability with the adaptation law is analyzed using a Lyapunov-based approach. Numerical simulations for the non-affine system of morphing aircraft are carried out to demonstrate the performance of the proposed scheme.

This paper is organized as follows. The problem considered in this study is stated in Sec. 2. Section 3 contains the control design process, and a solution for the adaptive frequency-apportioned control allocation problem. Numerical simulation result is shown in Sec. 4, and conclusions are given in Sec. 5.

2. Problem Statement

The morphing wing aircraft model considered in this study is shown in Fig. 1. Variable-span and variable-sweep morphing can be parameterized by two morphing parameters, η_1 and η_2. Span and sweep angle variations are linearly mapped onto $[-0.5, 0.5]$, as summerized in Table 1.

	Min. Span	**Max. Span**	**Min. Sweep**	**Max. Sweep**
Value	1.7 m	2.8 m	0 deg	40 deg
Variable	$\eta_1 = -0.5$	$\eta_1 = 0.5$	$\eta_2 = -0.5$	$\eta_2 = 0.5$

Table 1: Define morphing parameter.

2.1 Longitudinal Dynamic Model of Morphing Aircraft

In this study, the longitudinal motion of aircraft is considered. The nominal dynamic model is obtained at the flight condition of airspeed 20 m/s with the altitude 300 m, where both morphing parameters are zero. The longitudinal motion is governed by the following dynamic equations.

DOI: 10.13009/EUCASS2019-163

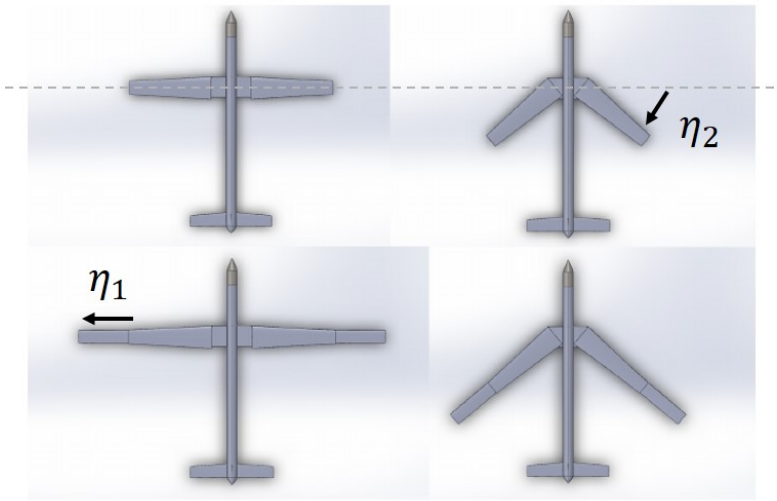

Figure 1: Morphing parameter definition.

$$\dot{V} = F_T \cos(\alpha + \alpha_T) - D(x,u) - mg \sin\gamma \tag{1}$$

$$m\dot{\gamma}V = F_T \sin(\alpha + \alpha_T) + L(x,u) - mg \cos\gamma \tag{2}$$

$$\dot{\alpha} = q - \gamma \tag{3}$$

$$\dot{q} = M/J_y(u) \tag{4}$$

The state variables are airspeed V, angle of attack α, pitch rate q, and flight path angle γ. The virtual control variables are thrust force F_T, and aerodynamic moments M which represent the desired dynamics for tracking control. The desired dynamics are distributed to the control variables which are throttle command δ_t, elevator deflection δ_e, and morphing parameters η_1, η_2. It is assumed that the dynamic model is not affine in control input system, but is represented as non-affine in the control input system. By considering the morphing parameters as control effectors, the dynamic model of the system can be represented as a non-affine form in control input. It can be shown that the dynamic nonlinearities in the morphing aircraft are dependent not only on the states of the system but also on the control inputs. The dynamic model can be represented as

$$\dot{x} = f(x,u) \tag{5}$$

where x is a state vector, and u is a control input vector.

2.2 Augmented Dynamic Model

To design a controller for the non-affine in the control input system, Eq. (5) is differentiated with respect to time so that $\dot{u}$ appears linearly in the resulting equation. The resulting model transforms the original model to affine in new control system without any approximation.

$$\ddot{x} = \frac{\partial f(x,u)}{\partial x}\dot{x} + \frac{\partial f(x,u)}{\partial u}\dot{u} \tag{6}$$

The augmented dynamic model is represented affine in virtual control input. For the non-affine system, by using the augmented dynamic model, the algebraic loop problem can be avoided, which is a general problem in the control algorithm of the non-affine system.

3. Control Design

In this section, a control system is designed so that the closed-loop system asymptotically tracks a smooth prescribed trajectory $X_{ref} = [V_{ref}, \gamma_{ref}]^T$. It is assumed that the reference trajectory $X_{ref} = [V_{ref}, \gamma_{ref}]^T$ is differentiable. Due to the problem that inverse dynamics does not exist, which is known as the non-minimum phase phenomenon, it is not easy to design a controller that tracks the reference trajectory by dynamic inversion. Thus, in this study, the control law

DOI: 10.13009/EUCASS2019-163

is designed based on three loop feedback design for a cascaded form by decomposing the control system, and control allocation method is utilized. The proposed control system is briefly depicted as a block diagram in Fig. 2. State and control variables for each loop are defined as follows,

$$X = \left[X_1^T, X_2^T, X_3^T\right]^T \tag{7}$$

where

$$X_1 = \left[V, \gamma\right]^T \tag{8}$$

$$X_2 = \alpha \tag{9}$$

$$X_3 = q \tag{10}$$

3.1 Baseline Control Law

The control design is decomposed in three feedback-loop designs. The nonsingularity of the inverse model of each loop can be proved by the following theorem.

Theorem 1 (Implicit function theorem) *Assume that $f_1, \ldots, f_n$ are differentiable functions on a neighborhood of the point*
$(x_0, y_0) = (x_1^0, \ldots, x_n^0, y_1^0, \ldots, y_n^0)$ *in* $\mathbb{R}^n \times \mathbb{R}^m$*, for trim conditions* $f_1(x_0, y_0) = f_2(x_0, y_0) = \ldots = f_n(x_0, y_0) = 0$*, and if the* $n \times n$ *matrix*

$$\begin{pmatrix} \frac{\partial f_1}{\partial x_1} & \frac{\partial f_1}{\partial x_2} & \cdots & \frac{\partial f_1}{\partial x_n} \\ \frac{\partial f_2}{\partial x_1} & \frac{\partial f_2}{\partial x_2} & \cdots & \frac{\partial f_2}{\partial x_n} \\ \vdots & \vdots & \ddots & \vdots \\ \frac{\partial f_n}{\partial x_1} & \frac{\partial f_n}{\partial x_2} & \cdots & \frac{\partial f_n}{\partial x_n} \end{pmatrix} \tag{11}$$

is nonsingular at (x_0, y_0)*, then there exists a neighborhood U of the point* $y_0 = (y_1^0, \ldots, y_m^0)$ *in* $\mathbb{R}^m$*, a neighborhood V of the point* $x_0 = (x_1^0, \ldots, x_n^0)$ *in* $\mathbb{R}^n$*, and a unique mapping* $\varphi : U \to V$ *such that* $\varphi(y_0) = x_0$ *and* $f_1(\varphi(y), y) = \ldots = f_n(\varphi(y), y) = 0$ *for all y in U. Furthermore,* φ *is differentiable.*

The control law of each loop is proposed as

$$\dot{u} = \left(\frac{\partial f(x,u)}{\partial u}\right)^{-1} \left(-\frac{\partial f(x,u)}{\partial x} f(x,u) + v\right) \tag{12}$$

Equation (12) results in $\ddot{x} = v$, where v can now be chosen to have the desired dynamics of the closed-loop system. For instance, if x_{ref} is continuously differentiable, v can be chosen as

$$v = \ddot{x}_{ref} - k_1(x - x_{ref}) - k_2(\dot{x} - \dot{x}_{ref}) \tag{13}$$

where $k_1 > 0$, and $k_2 > 0$. Let $e = x - x_{ref}$, then the closed-loop system is governed by $\ddot{e} + k_2\dot{e} + k_1 e = 0$, which means that the tracking objective is achieved exponentially.

Controller 1. The objective of the first-loop controller is to control V and γ to the desired values. The available virtual controls in this step are the aerodynamic angle α and the thrust force F_T.

$$\begin{bmatrix} V \\ \gamma \end{bmatrix} \Rightarrow \begin{bmatrix} F_T \\ \alpha \end{bmatrix} \tag{14}$$

Thus, $X_{2,des} = \alpha$ and its derivatives can be obtained by Eq. (12).

Controller 2. The reference signal $X_{2,des} = \alpha$ and its derivative can be found in the first-loop. The available virtual control in the second-loop controller is the angular rates q.

$$\left[\alpha\right] \Rightarrow \left[q\right] \tag{15}$$

DOI: 10.13009/EUCASS2019-163

Thus, $X_{3,des} = q$ and its derivatives can be obtained by Eq. (12).

Controller 3. In the final loop, the reference signal $X_{3,des} = q$ and its derivative can be found in the previous loop, and the next feedback loop can be determined. The available virtual control in this step is the aerodynamic moment M.

$$\left[q\right] \Rightarrow \left[M\right] \tag{16}$$

Thus, the derivatives of the virtual control $\dot{u}_{virtual}$ can be obtained from Eq. (12), and the virtual control $u_{virtual} = \left[F_T, M\right]^T$ can be found by integration.

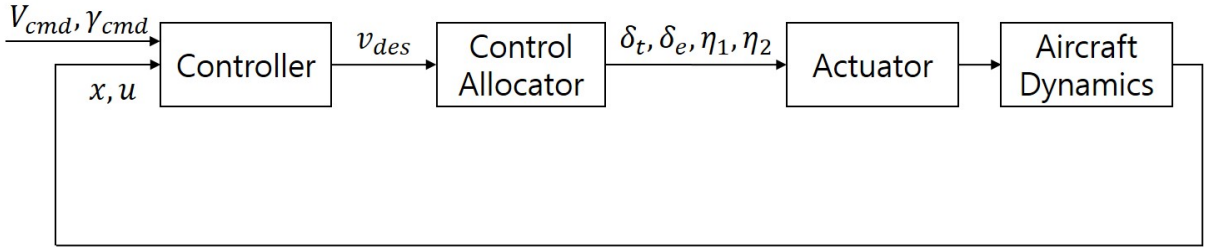

Figure 2: Block diagram of the control system.

3.2 Control Allocation

In this study, control allocation method is adopted to distribute the desired total forces and moments to the control effectors. The control allocation method has been widely used for the control effect distribution of redundantly actuated systems. The dynamics of morphing aircraft considered in this study is an over-actuated system by augmenting the control input with morphing parameters. The optimal control effect distribution can be determined by using control allocation to provide the desired forces and moments. Note that the morphing parameters generally change slowly compared to the conventional control surfaces. Therefore, the rate difference between actuators should be considered to guarantee control performance. In this study, the frequency-apportioned control allocation method is adopted to determine control distribution. The high-frequency component of the commands is allocated to the conventional control surfaces, and the low-frequency component of the commands is allocated to the morphing parameters. An adaptation law is used to compensate for the allocation error caused by the time-varying control effectiveness matrix. Let us define the virtual control as $v_{des} = u_{virtual}$.

Weighted Pseudo Inverse. The CA problem is to find the control vector u, $u \in \mathbb{R}^m$, such that

$$\mathbf{B}u = v_{des} \tag{17}$$

subject to

$$u_{min} \leq u \leq u_{max} \tag{18}$$

where $v_{des} = [F_T, M]^T$ is the desired forces and moment, and $\mathbf{B}$ is the control effectiveness matrix of the following form.

$$\mathbf{B} = \begin{pmatrix} \frac{\partial F_T}{\partial \delta_1} & \frac{\partial F_T}{\partial \delta_2} & \frac{\partial F_T}{\partial \delta_3} & \frac{\partial F_T}{\partial \delta_4} \\ \frac{\partial M}{\partial \delta_1} & \frac{\partial M}{\partial \delta_2} & \frac{\partial M}{\partial \delta_3} & \frac{\partial M}{\partial \delta_4} \end{pmatrix}, \quad \mathbf{B} \in \mathbb{R}^{l \times m} \tag{19}$$

Note that for the over-actuated systems, the number of columns of $\mathbf{B}$ is greater than the number of rows of $\mathbf{B}$ and has full column rank. The weighted pseudo-inverse method is used for the control allocation, which requires a pseudo-inversion of the non-square matrix $\mathbf{B}$. The solution is obtained analytically by solving the following optimization problem.

$$\begin{aligned} &minimize \quad J = \frac{1}{2}(u + c)^T W(u + c) \\ &subject\ to \quad \mathbf{B}u = v_{des} \end{aligned} \tag{20}$$

The solution is obtained as follows,

$$u = -c + \mathbf{B}^{\dagger}\left(v_{des} + \mathbf{B}c\right) \tag{21}$$

DOI: 10.13009/EUCASS2019-163

where c is the offset to consider the saturation of control effectors, and $\mathbf{B}^{\dagger}$ is the weighted pseudo-inversion of $\mathbf{B}$ as follows,

$$\mathbf{B}^{\dagger} = W^{-1}\mathbf{B}^{T}\left(\mathbf{B}W^{-1}\mathbf{B}^{T}\right)^{-1} \tag{22}$$

where W is a diagonal positive definite weighting matrix which is chosen by considering the saturation of the control effectors.

3.2.1 Frequency-Apportioned Control Allocation

The actuator rate limits should be considered to guarantee the control performance of the slowly varying actuator system. The FACA method distributes the high-frequency component of the commands to the control effectors with higher rate limits which would be conventional control surfaces, and the low-frequency component of the commands to the control effectors with lower rate limits which would be morphing parameters. The block diagram of the frequency-apportioned control allocation method is shown in Fig. 3. The distribution is implemented by using a low-pass filter (LPF), and the distributed desired forces and moment with low-frequency and high-frequency are represented as follows,

$$v_h = L(s)v_{des} \tag{23}$$

$$v_l = \left(1 - L(s)\right)v_{des} \tag{24}$$

where the LPF is represented as

$$L(s) = \frac{1}{\tau_c s + 1} \tag{25}$$

The time constant τ_c is determined to separate the u_h and the u_l. Consequently, the control vector can be obtained as

$$u = u_h + u_l = \left(\mathbf{B}_h^{\dagger}\left(1 - L(s)\right) + \mathbf{B}_l^{\dagger}L(s)\right)v_{des} \tag{26}$$

where $\mathbf{B}_h^{\dagger}$ and $\mathbf{B}_l^{\dagger}$ are the high and low-frequency weighted pseudo-inverse, respectively, and the control variables are throttle δ_t, elevator angle δ_e, and morphing parameters η_1 and η_2, respectively.

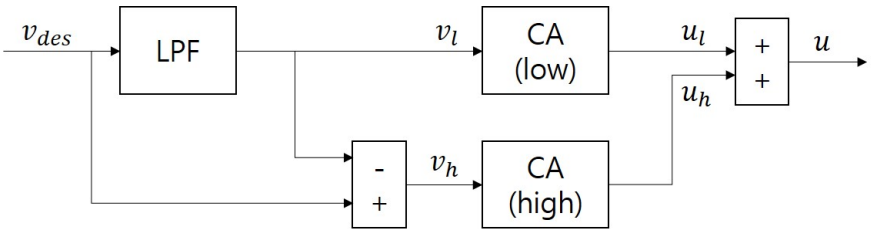

Figure 3: Frequency-Apportioned Control Allocation.

3.2.2 Adaptation Law

In general, There exists errors in the nominal control effectiveness matrix. For the non-affine in control input system, the allocation error will be inevitably caused by the difference between the real and the nominal control effectiveness matrices, and by the frequency-apportioned control allocation. Therefore, it is necessary to propose a new control allocation method to eliminate the allocation error. To deal with this problem, the following adaptation law is considered.

$$v_r = \mathbf{B}^{*}\mathbf{B}^{\dagger}\left(v_{des} + v_c\right) \tag{27}$$

where $\mathbf{B}^{*}$ represents the true control effectiveness matrix, which may be the sum of nominal control effectiveness matrix and uncertainty. Let us define the allocation error as

$$e_v = v_{des} - v_r \tag{28}$$

DOI: 10.13009/EUCASS2019-163

where v_r is the real value of the desired force and moment. In Ref. 24, the control allocation method is considered as a discrete system, although it is a continuous system. To realize the continuous system and compensate the error induced by the control input, a first-order low-pass filter is introduced, which is modeled as follows,

$$\dot{v}_c = \tau\left(v_{cp} - v_c\right) \tag{29}$$

where v_c is the compensating value of desired force and moment. Then, the error dynamics can be represented as follows,

$$\dot{e}_v = \dot{g} - \mathbf{B}^*\mathbf{B}^\dagger\tau v_{cp} + \mathbf{B}^*\mathbf{B}^\dagger\tau v_c \tag{30}$$

where

$$\dot{g} = \frac{d}{dt}\left(\left(I - \mathbf{B}^*\mathbf{B}^\dagger\right)v_d\right) - \frac{d}{dt}\left(\mathbf{B}^*\mathbf{B}^\dagger\right)v_c \tag{31}$$

By adapting this approach, the adaptation law of the compensation term v_{cp} can be chosen as

$$v_{cp} = \left(\mathbf{B}^*\mathbf{B}^\dagger\right)^{-1}\left(\mathbf{B}^*\mathbf{B}^\dagger\tau v_c - \dot{g} - k_3 e_v\right) \tag{32}$$

3.2.3 Closed-loop Stability Analysis

Substituting the adaptive law in Eq. (32) into Eq. (30) , the error dynamics can be written as follows,

$$\dot{e}_v + k_3 e_v = 0 \tag{33}$$

where τ and k_3 are positive constants, and τ should be chosen as large as enough. Note from Eq. (33) that the closed-loop system stability is guaranteed by stabilizing the error dynamics in the sense of Lyapunov. Finally, it can be shown that the allocation error e_v tends to zero as t goes to infinity.

4. Numerical Simulation

Numerical simulation is performed to demonstrate the performance of the proposed control law. In this study, the variable-span and variable-sweep morphing wing aircraft is modeled as a non-affine in control input and nonlinear system. The actuator dynamics are modeled considering the saturation of the actuator, and the simulation time is set to 50 seconds. The initial flight condition is a trim condition with $V = 20\ m/s$ at $h = 300\ m$. Simulations are conducted for the airspeed tracking and flight path angle tracking. To generate a differentiable command signal, the reference command is transferred to the controller through the command filter.

4.1 Baseline Control Law with Frequency-Apportioned Control Allocation

Simulation results are shown in Fig. 4-11. Figures 4, 6, and 8 show the resulting state trajectories for the different scenarios of the flight path angle tracking and the reference command signals. Figures 5, 7, and 9 show the corresponding control input trajectories, respectively. It can be shown that all the flight path angle tracking scenarios are achieved with the control design for the non-affine in control input system. Also, the airspeed tracking performance is shown in Fig. 10, the state trajectories, and Fig. 11, the control input trajectories. It is seen that the response is acceptable and the control objective is achieved with all control inputs within the saturation bounds, while the frequency rate bounds of the morphing parameters are satisfied.

4.2 Adaptive Frequency-Apportioned Control Allocation

The simulation results of FACA are shown in Figs. 12-17. According to the cutoff-frequency, the control effect is distributed high and low-frequency components to each control effectors. As shown in Figs. 12 and 13, the elevator has high-frequency component and the morphing parameters have low-frequency component. As the cutoff-frequency of LPF increases, the elevator has more high-frequency component, while achieving the desired objective. The state and control trajectories of the system with the adaptive FACA are shown in Figs. 14-17. The non-adaptive controller is compared with the adaptive controller for the non-affine in control input system about the system with small uncertainty to identify the robustness of the adaptive control design. In this study, to focus on the performance of the system with uncertainty, only the flight path angle tracking is considered as the simulation scenario. Figures. 14 and 16 show that

DOI: 10.13009/EUCASS2019-163

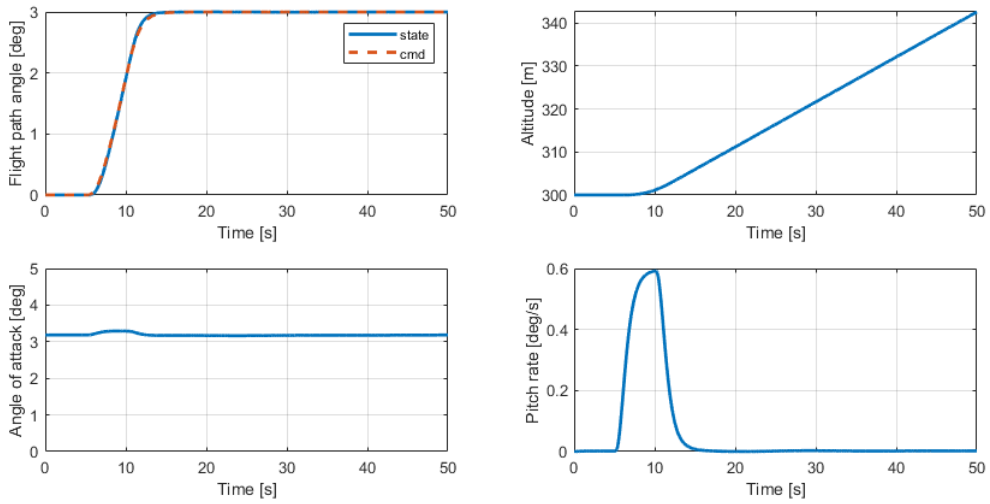

Figure 4: Flight path angle tracking responses - scenario1.

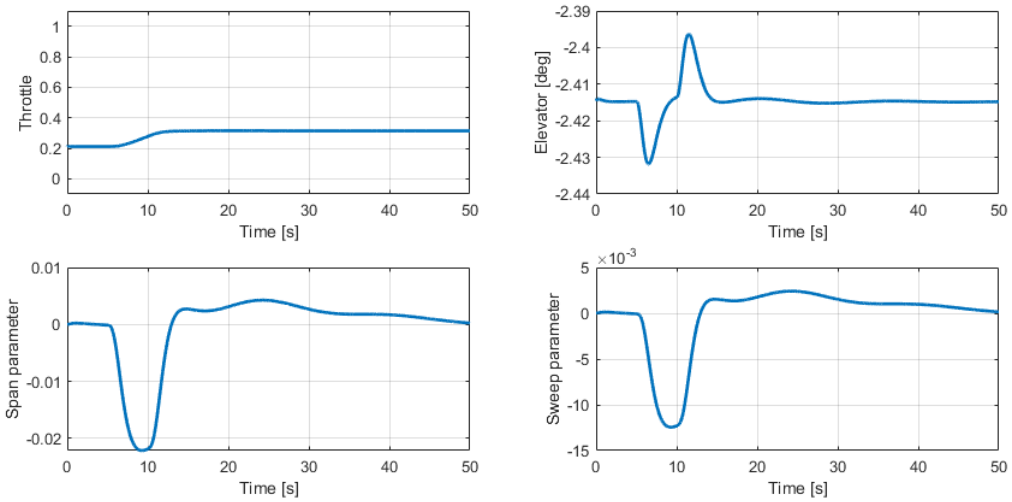

Figure 5: Control input responses.

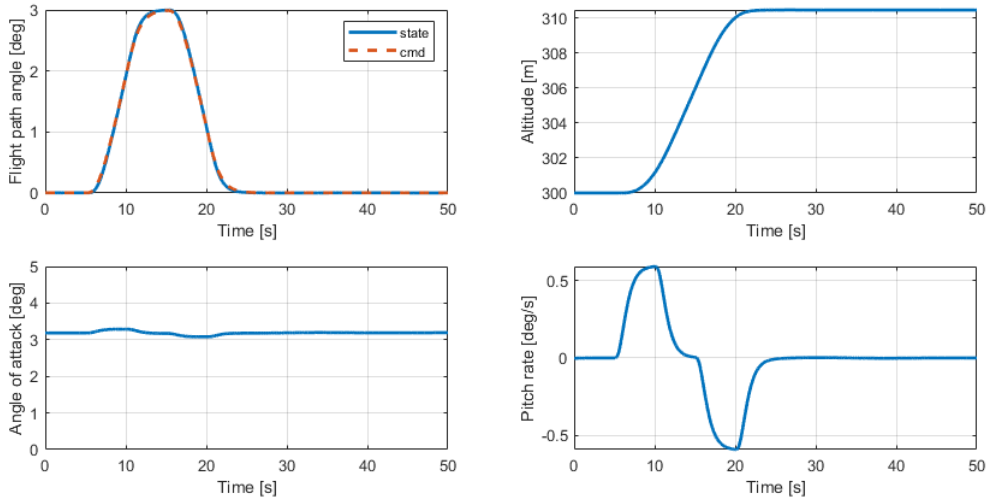

Figure 6: Flight path angle tracking responses - scenario2.

DOI: 10.13009/EUCASS2019-163

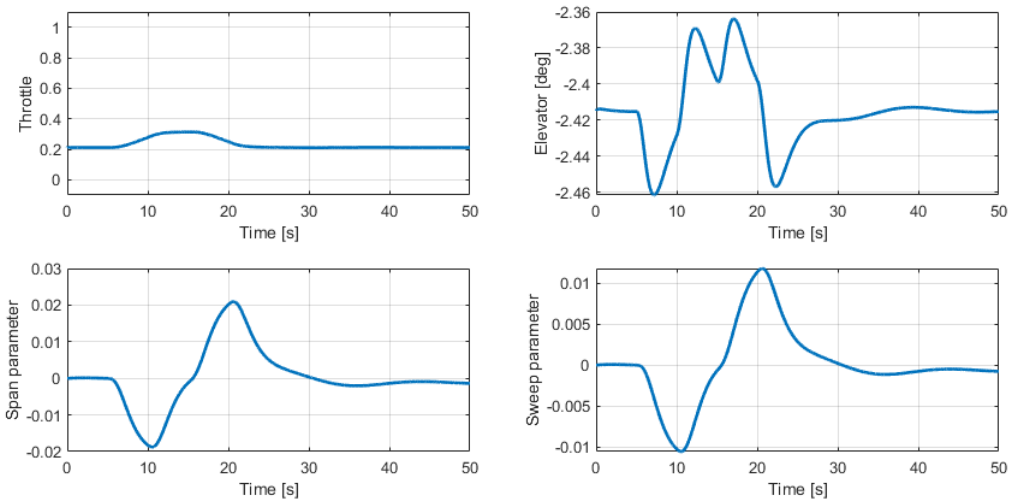

Figure 7: Control input responses.

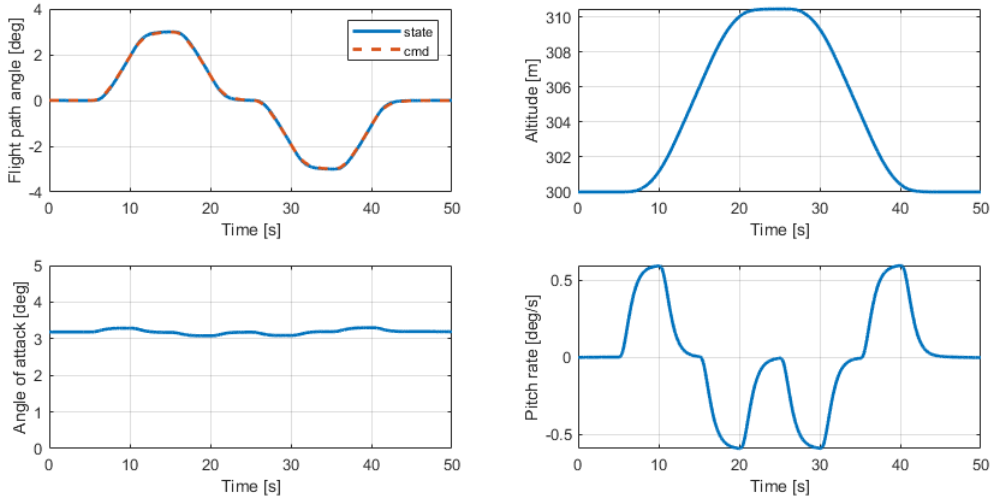

Figure 8: Flight path angle tracking responses - scenario3.

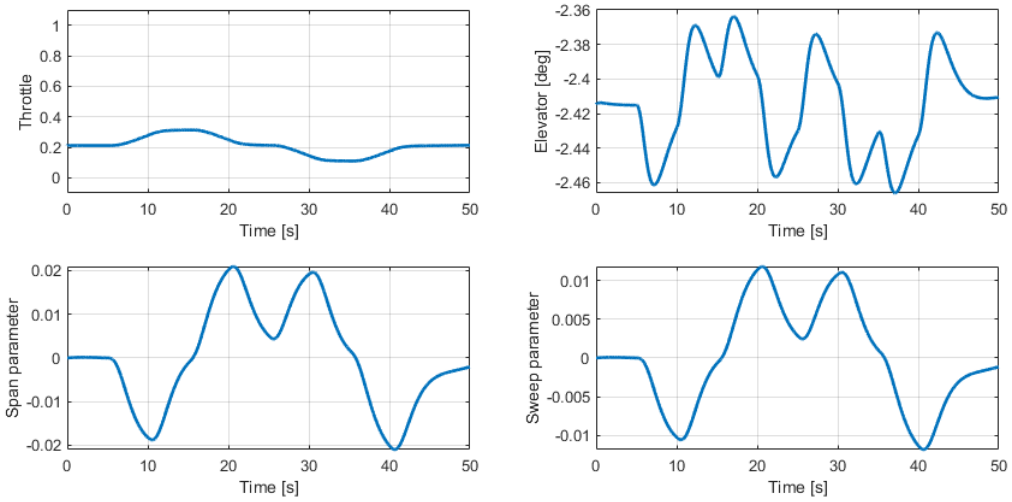

Figure 9: Control input responses.

DOI: 10.13009/EUCASS2019-163

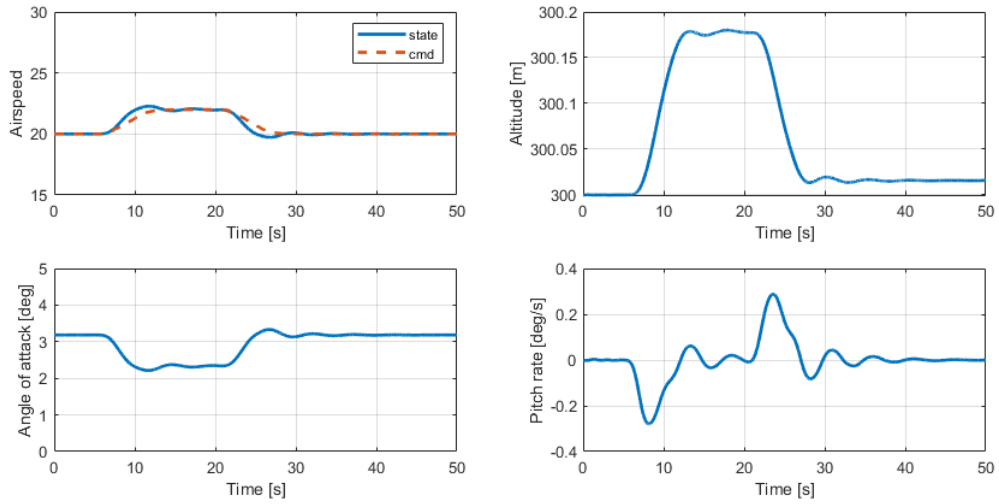

Figure 10: Airspeed tracking responses.

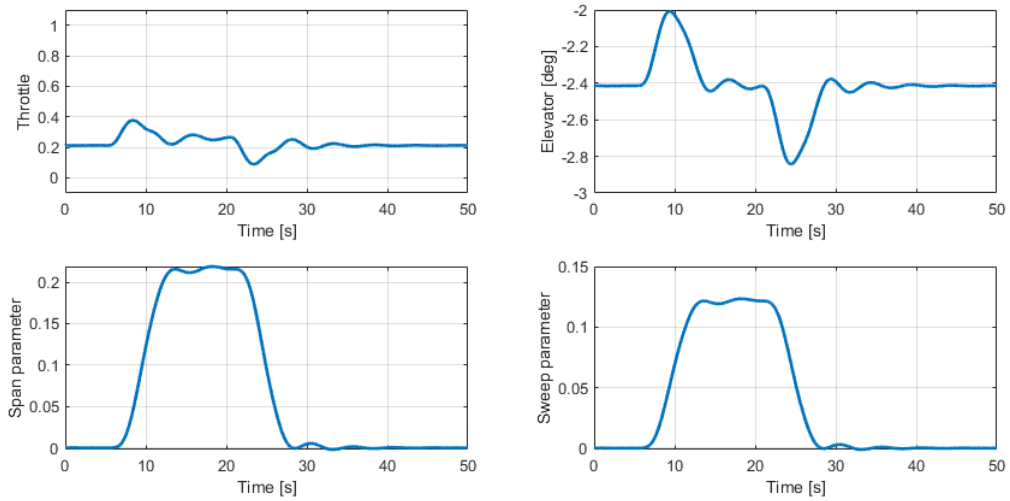

Figure 11: Control input responses.

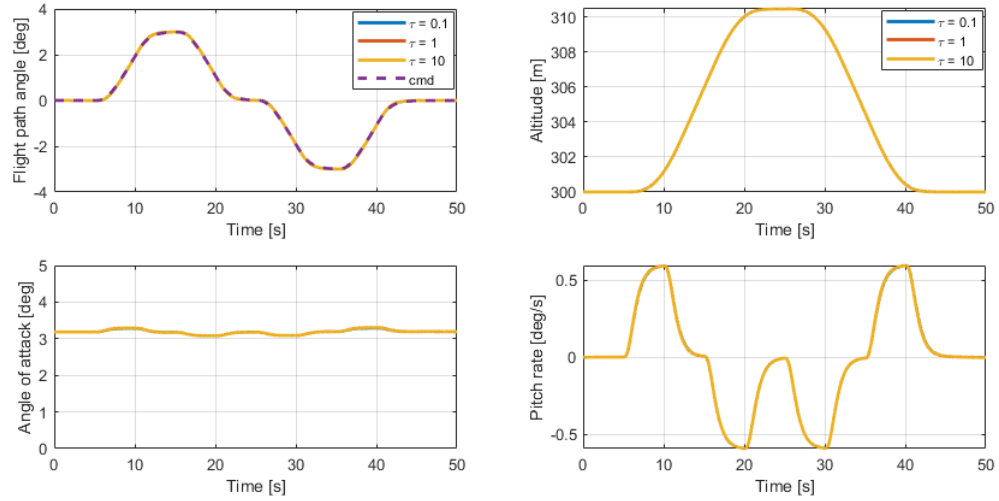

Figure 12: FACA results at several cutoff-frequency.

DOI: 10.13009/EUCASS2019-163

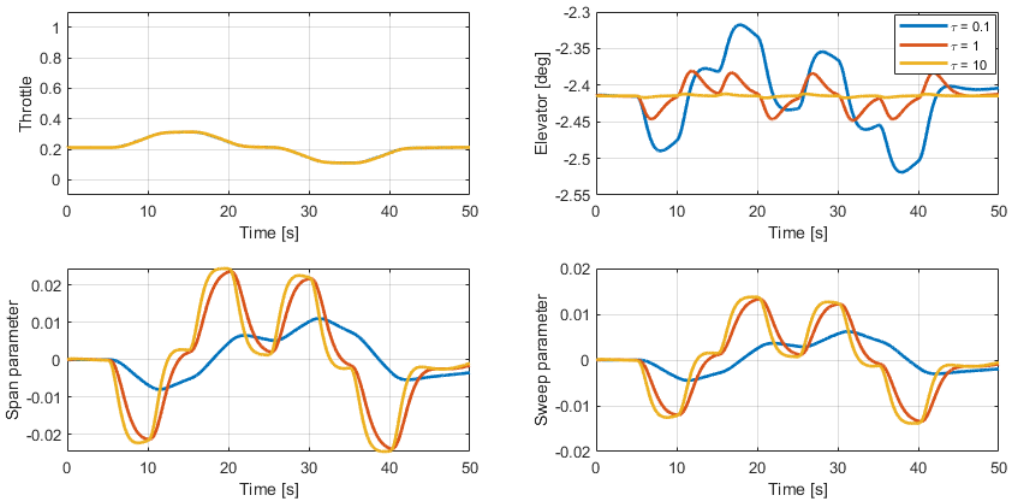

Figure 13: Control input responses.

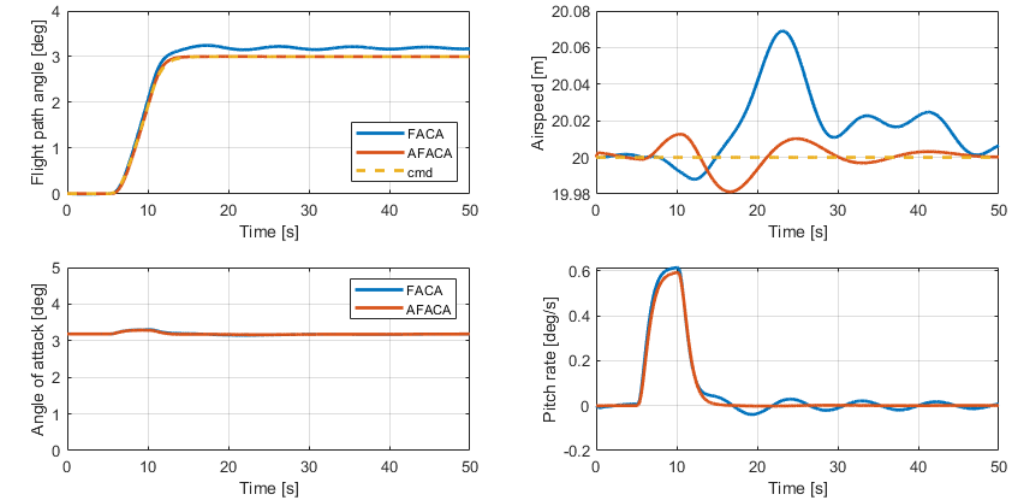

Figure 14: FACA vs. AFACA with 10% uncertainty.

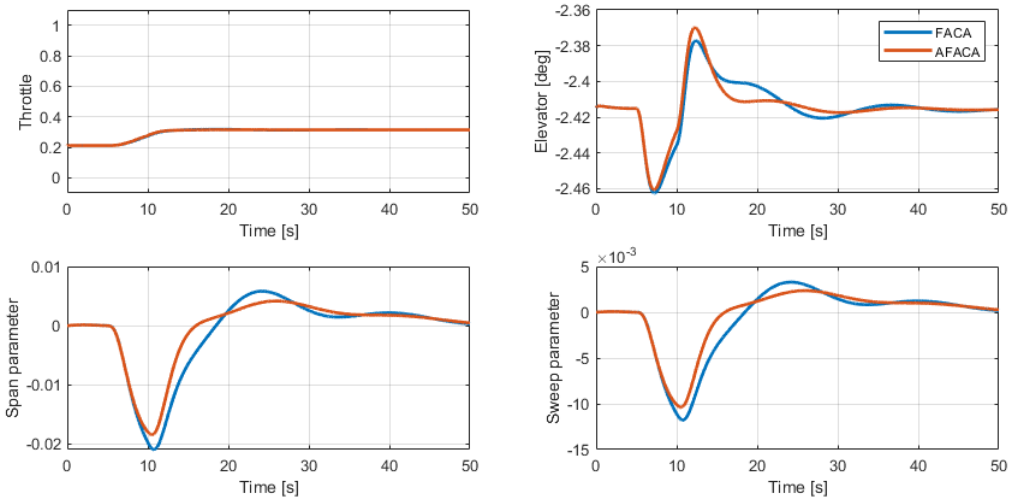

Figure 15: Control input responses.

DOI: 10.13009/EUCASS2019-163

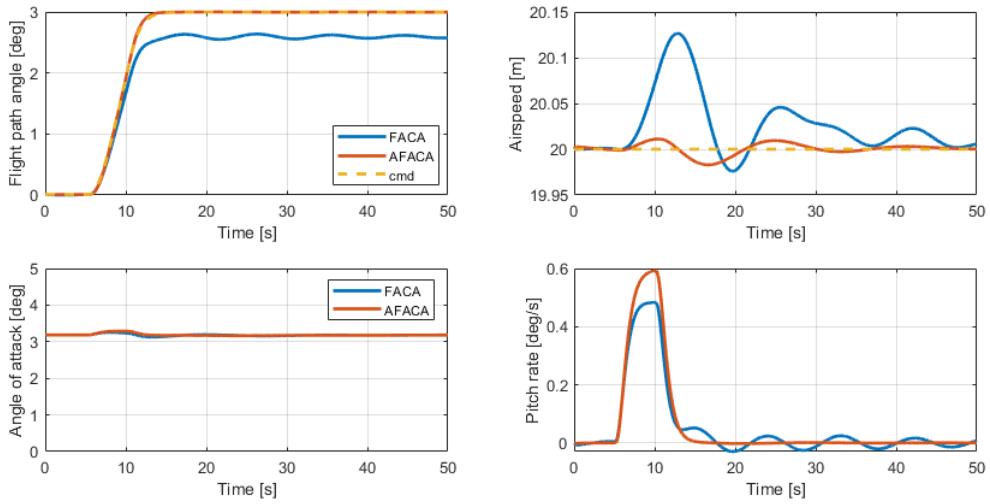

Figure 16: FACA vs. AFACA with 20% uncertainty.

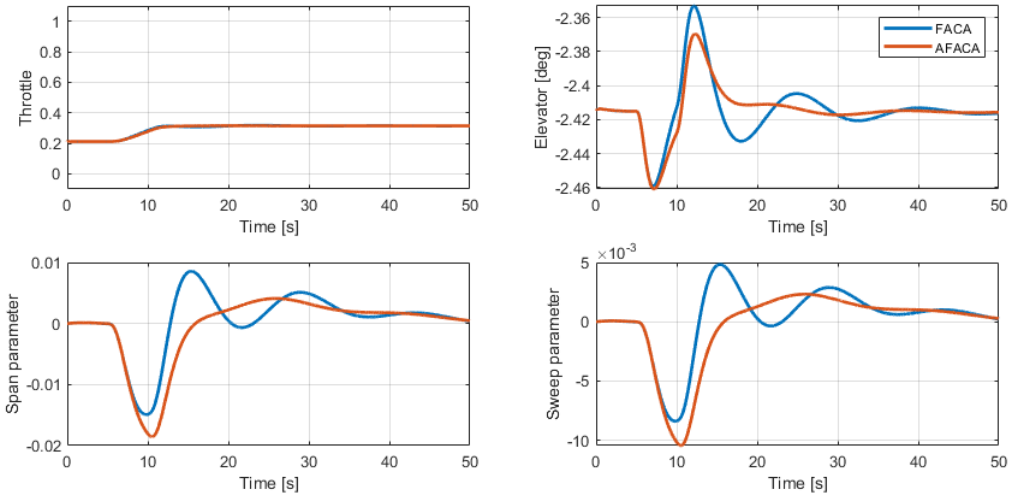

Figure 17: Control input responses.

the error caused by the system uncertainty converges to zero, when using the adaptive non-affine controller. However, when using the non-adaptive non-affine controller, the error caused by the system uncertainty does not converge to zero.

In summary, considering the variation of system dynamics of the morphing parameters as the non-affine in control input system design, the fidelity and operational performance are improved, while covering the frequency difference of the conventional flap and morphing actuators and the rate limits of morphing parameters. Note that the reference signals are transferred to the controller through an appropriate command filter to generate the differentiable command signal.

5. Conclusion

Control design strategy for the non-affine in control input system of a variable-span and variable-sweep morphing wing aircraft was proposed based on the adaptive frequency-apportioned control allocation. The dynamic model of the morphing aircraft, represented by the non-affine in control input system, was transformed into an affine in control input form without any approximation. When solving the flight-path angle tracking problem with control surfaces, the non-minimum phase issue appears, which may lead the system to be unstable. In this study, the cascade control design was applied by decomposing the control law in three feedback loop. The required control efforts were distributed via

DOI: 10.13009/EUCASS2019-163

the frequency-apportioned control allocation method to account for the low bandwidth of the morphing actuators. The nonlinear system for which the method is applicable was assumed to be of the known order, however, it may contain unmodeled dynamics or parameter uncertainty. The stability of the proposed control law with adaptation rule was proved by Lyapunov theory. Numerical simulation was conducted to demonstrate the effectiveness of the proposed approach by applying to the non-affine morphing aircraft. Simulation results showed that the proposed controller achieved good tracking performance with the adaptation law, even when the system uncertainty exists.
For the future studies, the lateral motion will be considered. Combining the lateral motion with longitudinal motion, the coupling motion of the forces and moments may extend the flight envelope. The proposed control scheme can be applied to fault-tolerant controller due to the increased degree of freedom of control effectors.

6. Acknowledgments

This work was supported by the R&D Program in Aerospace Parts and Materials (10066055) through the Korea Evaluation Institute of Industrial Technology funded by the Ministry of Trade, Industry, and Energy, Republic of Korea.

References

[1] N. Prabhakar, R. J. Prazenica, and S. Gudmundsson, "Dynamic analysis of a variable-span, variable-sweep morphing UAV," *IEEE Aerospace Conference*, Big Sky, MT, March 2015.

[2] N. Prabhakar, R. J. Prazenica, S. Gudmundsson, and M. J. Balas, "Transient dynamic analysis and control of a morphing UAV," *AIAA Guidance, Navigation, and Control Conference*, San Diego, CA, January 2016.

[3] B. Bai and C. Dong, "Modeling and LQR switch control of morphing aircraft," *Sixth International Symposium on Computational Intelligence and Design*, Hangzhou, China, October 2013.

[4] J. Valasek, A. Lampton, and M. Marwaha, "Morphing unmanned air vehicle intelligent shape and flight control," *AIAA Infotech@Aerospace Conference*, Seattle, WA, April 2009.

[5] A. Hurst, A. Wickenheiser, and E. Garcia, "Control of an adaptive aircraft with a morphing input," *AIAA/ASME/ASCE/AHS/ASC Structures, Structural Dynamics, and Materials Conference*, Palm Springs, CA, May 2009.

[6] A. Isidori, *Nonlinear Control Systems*. Communications and Control Engineering, Springer, London, UK, 2013.

[7] K. Boothe, K. Fitzpatrick, and R. Lind, "Controllers for disturbance rejection for a linear input-varying class of morphing aircraft," *AIAA/ASME/ASCE/AHS/ASC Structures, Structural Dynamics, and Materials Conference*, Austin, TX, April 2005.

[8] A. Young, C. Cao, N. Hovakirnyan, and E. Lavretsky, "An adaptive approach to nonaffine control design for aircraft applications," *AIAA Guidance, Navigation, and Control Conference*, Keystone, CO, August 2006.

[9] C. Ahn, Y. Kim, and H. Kim, "Adaptive sliding mode control for non-affine nonlinear vehicle systems," *AIAA Guidance, Navigation, and Control Conference*, Hilton Head, SC, August 2007.

[10] R. Choe, E. Xargay, and N. Hovakimyan, "L1 adaptive control for a class of uncertain nonaffine-in-control nonlinear systems," *IEEE Transactions on Automatic Control*, vol. 61, no. 3, pp. 840–846, 2016.

[11] B. Yang and A. J. Calise, "Adaptive control of a class of nonaffine systems using neural networks," *IEEE Transactions on Neural Networks*, vol. 18, no. 4, pp. 1149–1159, 2007.

[12] J. Zhang and S. T. Wu, "Dynamic modeling and control for a morphing aircraft," *The 26th Chinese Control and Decision Conference*, Changsha, China, July 2014.

[13] N. Hovakimyan, E. Lavretsky, and A. Sasane, "Dynamic inversion for non affine-in-control systems via time-scale separation. part I," *Journal of Dynamical and Control Systems*, vol. 13, no. 4, pp. 451–465, 2007.

[14] E. Lavretsky and N. Hovakimyan, "Adaptive dynamic inversion for nonaffine-in-control uncertain systems via time-scale separation. part II," *Journal of Dynamical and Control Systems*, vol. 14, no. 1, pp. 33–41, 2008.

[15] J. D. Boskovic, L. Chen, and R. K. Mehra, "Adaptive control design for nonaffine models arising in flight control," *Journal of Guidance, Control, and Dynamics*, vol. 27, no. 2, pp. 209–217, 2004.

DOI: 10.13009/EUCASS2019-163

[16] B. D. Craven, "Implicit function theorems and lagrange multipliers," *Numerical Functional Analysis and Optimization*, vol. 2, no. 6, pp. 473–486, 1980.

[17] S. H. Lane and R. F. Stengel, "Flight control design using non-linear inverse dynamics," *Automatica*, vol. 24, no. 4, pp. 471–483, 1988.

[18] R. M. Hirschorn, "Invertibility of nonlinear control systems," *SIAM Journal on Control and Optimization*, vol. 17, no. 2, pp. 289–297, 2005.

[19] T. A. Johansen and T. I. Fossen, "Control allocation - a survey," *Automatica*, vol. 49, no. 5, pp. 1087–1103, 2013.

[20] W. C. Durham, "Constrained control allocation," *Journal of Guidance, Control, and Dynamics*, vol. 16, no. 4, pp. 717–725, 1993.

[21] M. W. Oppenheimer, D. B. Doman, and M. A. Bolender, "Control allocation for over-actuated systems," *14th Mediterranean Conference on Control and Automation*, Ancona, Italy, August 2006.

[22] J. B. Davidson, F. J. Lallman, and W. T. Bundick, "Integrated reconfigurable control allocation," *AIAA Guidance, Navigation, and Control Conference*, Montreal,Canada, August 2001.

[23] Y. Zhang and Z. Chen, "A closed-loop control allocation method for satellite precision pointing," *IEEE 10th International Conference on Industrial Informatics*, Beijing, China, July 2012.

[24] Q. Hu, X. Tan, and M. R. Akella, "Closed-loop-based control allocation for spacecraft attitude stabilization with actuator fault," *Journal of Guidance, Control, and Dynamics*, vol. 41, no. 4, pp. 944–953, 2018.